Canadian Mineralogist
Vol. 28, pp. 287-298 (1990)

PRESSURE–TEMPERATURE CONSTRAINTS ON THE CRYSTALLIZATION OF THE HARDING PEGMATITE, TAOS COUNTY, NEW MEXICO

BRYAN C. CHAKOUMAKOS* AND GREGORY R. LUMPKIN**
Department of Geology, University of New Mexico, Albuquerque, New Mexico 87131, U.S.A.

ABSTRACT

A *P–T* path for the crystallization of the Harding pegmatite magma has been constrained from 1) the experimentally determined liquidus, solidus and phase assemblages for a bulk sample of the pegmatite, 2) isochores for CO_2–H_2O–NaCl fluid inclusions in quartz and beryl from the various lithologic units of the pegmatite, 3) the conditions of metamorphism of the surrounding host-rock, and 4) pegmatite mineral equilibria, including the Li–Al-silicates, micas, and feldspars. The magmatic portion of crystallization began at 650°C and 330–350 MPa (11–12 km depth) and continued isobarically to 550°C. Fluid inclusions indicate that the fluid composition (mole %) evolved from $6CO_2$:4NaCl to less than $1CO_2$:10NaCl during the crystallization. If the host-rock temperature at the time of intrusion was 0 to 200°C below the solidus temperature, then cooling models for a finite sheet indicate that the magmatic crystallization (giant-crystal texture) occurred in 1000 years or less. The subsolidus hydrothermal replacement and re-equilibration continued for several million years. Isobaric cooling continued to 400–300°C, followed by uplift and erosion. Given the estimated age and depth of the pegmatite, then the average rate of uplift of the Picuris Range was 0.7 – 1.0 cm/yr. Li–Be-bearing margarite, prominent in the hanging-wall metasomatic aureole, probably crystallized below the pegmatite solidus. Quartz-spodumene intergrowths exposed in footwall aplite are interpreted as pseudomorphic replacements of early-formed petalite. Eucryptite replacement of spodumene occurred during uplift at 100–200°C.

Keywords: *P–T* crystallization path, granitic pegmatite, regional metamorphism, Li–Al silicates, petalite pseudomorphs, Li–Be-bearing margarite, fluid inclusions, cooling models, Proterozoic rocks, Harding pegmatite, New Mexico.

SOMMAIRE

Nous avons déterminé la pression et la température de cristallisation du magma qui a donné la pegmatite de Harding, au Nouveau-Mexique, à partir des contraintes suivantes: 1) le liquidus, le solidus, et les relations des phases, déterminés expérimentalement sur un échantillon de la pegmatite, 2) les isochores des inclusions fluides à CO_2–H_2O–NaCl dans le quartz et le béryl des diverses unités lithologiques de la pegmatite, 3) les conditions métamorphiques des roches encaissantes, et 4) les équilibres parmi les minéraux de la pegmatite, dont les silicates de Li–Al, les micas et les feldspaths. L'étape magmatique de la cristallisation a débuté à 650°C et 330–350 MPa (ce qui équivaut à 11–12 km de profondeur), et a continué de façon isobare jusqu'à 550°C. Les inclusions fluides témoignent d'un changement graduel dans la composition de la phase fluide, de $6CO_2$:4NaCl à moins de $1CO_2$:10NaCl (termes molaires) au cours de la cristallisation. En supposant que les roches encaissantes au moment de la mise en place avaient une température entre 0 et 200°C au dessous du solidus, les modèles de refroidissement pour une couche de magma indiquent une cristallisation magmatique à texture très grossière en 1000 années ou moins. Les phénomènes de remplacement et de ré-équilibrage au stade hydrothermal ont continué pour plusieurs millions d'années. Le refroidissement isobare, qui a continué jusqu'à 400–300°C, s'est terminé par un événement de soulèvement et d'érosion. Vus l'âge protérozoïque et la profondeur de la pegmatite, le taux moyen de soulèvement dans la chaîne de Picuris serait de 0.7 à 1.0 cm/an. La margarite à Li–Be, qui est prominente dans l'auréole de contact supérieure de la pegmatite, a probablement cristallisé au dessous du solidus. Les intercroissances à quartz + spodumène dans l'aplite près de la base résulteraient d'une pseudomorphose de la pétalite, phase précoce. Le remplacement du spodumène par l'eucryptite a eu lieu au cours du soulèvement régional, à 100–200°C.

(Traduit par la Rédaction)

Mots-clés: *P* et *T* de cristallisation, pegmatite granitique, métamorphisme régional, silicates de Li–Al, pseudomorphes de pétalite, margarite à Li–Be, inclusions fluides, roches protérozoïques, Harding, Nouveau-Mexique.

INTRODUCTION

The published record of geological studies of the Harding pegmatites and the surrounding Picuris Range in Taos County, New Mexico, spans more than 60 years (see Jahns & Ewing 1976, 1977 for reviews). The main pegmatite displays dramatic internal zoning and is a past producer (1919–1958) of commercial lepidolite, beryl, spodumene and tantalum–niobium minerals. This paper presents a compilation of relevant published data, combined with new field observations, which constrain a pressure – temperature (*P–T*) path for the crystallization and uplift of the Harding pegmatite magma. We have used 1) the conditions of metamorphism of the

*Present address: Oak Ridge National Laboratory, Solid State Division, P.O. Box 2008, Oak Ridge, Tennessee 37831-6056, U.S.A.
**Present address: Australian Nuclear Science and Technology Organization, Materials Division, Menai, New South Wales 2234, Australia.

surrounding host-rocks; 2) the experimentally determined liquidus, solidus, and phase assemblages of a bulk sample of the pegmatite; 3) pegmatite mineral equilibria; and 4) isochores for fluid inclusions in beryl and quartz from various lithologic units of the pegmatite.

Location and General Geology

The Harding pegmatite is located in the Picuris Range, 10 km east of Dixon and 30 km southwest of Taos, in sec. 29, T23N, R11E, in Taos County. Proterozoic metamorphic rocks of the Picuris Range are divided, on the basis of contrasting lithologies, into the Ortega and Vadito groups. The debate over the relative ages of these two groups has not ended [Bauer (1984) gives a recent review]; however, they probably share similar primary ages of 1750 to 1650 Ma, as neighboring ranges for which geochronological studies have been made (Grambling 1986). The pegmatite intrudes the Vadito Group. The main dike is about 370 m long and up to 80 m wide in outcrop. The body is roughly tabular, with a maximum thickness of 25 m and an average plunge of 10°S (Jahns & Ewing 1976, 1977). Exposures occur primarily along the boundary between amphibolite (hanging wall) on the south and pelitic schists (footwall) on the north (Long 1974, Jahns & Ewing 1976, McCarty 1983). Bedding (S_0) and transposition layering (S_0/S_1) trend N8°E in Vadito rocks north of the pegmatite. The primary foliation is slaty cleavage or schistosity (S_2), which trends N10°W and intersects bedding at a low angle (Holcombe & Callender 1982, Bauer 1984). The pegmatite truncates S_0/S_1 and must postdate F_1 and F_2 folding.

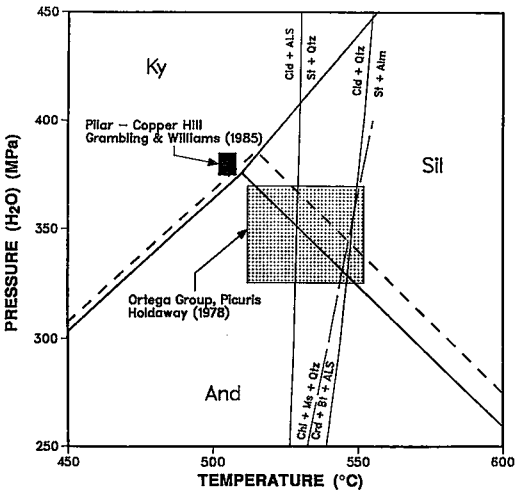

FIG. 1. A pressure – temperature diagram summarizing the relevant mineral equilibria and conditions of metamorphism for rocks of the Picuris Range. The equilibria curves for the aluminosilicates (bold solid lines) are according to Holdaway (1971), and the dashed curves show the effect of (Mn, Fe) solid solution in the aluminosilicates, as determined by Grambling & Williams (1985) for the rocks of the Picuris Range. Two curves (light solid lines) mark the introduction of staurolite, *i.e.*, chloritoid + aluminosilicate = staurolite + quartz, and chloritoid + quartz = staurolite + almandine (Ganguly 1969). Another curve (long dashes) marks the introduction of cordierite according to the reaction chlorite + muscovite + quartz = cordierite + biotite + aluminosilicate (Hirschberg & Winkler 1968). The two labeled boxes are ranges of metamorphic conditions estimated for rocks adjacent to and to the north of the Harding pegmatite terrane.

Several types of granitic rocks are present in the vicinity of the pegmatite. On the basis of field evidence and limited radiometric dating, Long (1974) considered the Harding pegmatite bodies to be late in the history of granitic magmatism in the area. He suggested a separate magmatic event for the pegmatites 100 Ma later than the youngest (unfoliated) granite and as much as 300–400 Ma later than the oldest (foliated) granitic rocks. Radiometric age determinations (Rb–Sr and K–Ar) for Harding samples are in the range 1495 to 1285 Ma for muscovite from the wall zone and 1335 to 1275 Ma for a whole-rock sample of the microcline – spodumene zone (Brookins *et al.* 1979, Clark 1982). Grambling (1986) speculated that the regional metamorphism and deformation of Proterozoic rocks in northern New Mexico occurred simultaneously at ~1410 Ma.

Constraints on T and P of Crystallization

Metamorphic equilibria

Geochronological studies (Brookins *et al.* 1979) and field relations (Long 1974, Jahns & Ewing 1976) indicate that the pegmatite is younger than the nearby plutons and deformation and metamorphism of the surrounding host-rock. The mineral assemblages and textures preserved in the pegmatite and its aureole show no evidence of regional deformation or metamorphism; therefore, the peak pressure experienced during metamorphism of the host rocks provides an upper bound on the pressure of emplacement and crystallization of the pegmatite magma. This is the first constraint that we shall discuss.

Rocks of the Vadito Group, which the Harding pegmatite intrudes, consist of interbedded amphibolites, metavolcaniclastic units, quartz–muscovite–biotite schists, and phyllites. Staurolite and cordierite are abundant in the pelitic units. The Al_2SiO_5 polymorphs are abundant throughout the Picuris Range; however, in the southernmost Vadito Group rocks, *i.e.*, around the Harding pegmatites, andalusite is found exclusively. Using data on aluminosilicate stability and garnet–biotite geothermometry, Grambling

& Williams (1985) estimated that kyanite-andalusite-sillimanite assemblages in the Pilar - Copper Hill area crystallized at 380 ± 5 MPa and 505 ± 3°C. From an analysis of mineral compositions and stability data for the aluminosilicates, staurolite and chloritoid, Holdaway (1978) estimated that the rocks of the Ortega Group similarly formed at 330 to 370 MPa and 532 ± 20°C. These estimates of the metamorphic conditions and relevant metamorphic equilibria for the Picuris range are summarized in Figure 1. Based on the occurrence of cordierite, staurolite and (the aluminosilicates restricted to) andalusite in the vicinity of the Harding pegmatite, we suggest that the peak metamorphic conditions for the Vadito Group rocks in the southern Picuris Range were 340 ± 10 MPa and 550 ± 10°C. The peak metamorphic pressure in the host rocks places an upper bound of 350 MPa for the pressure of emplacement of the magma that led to the Harding pegmatite.

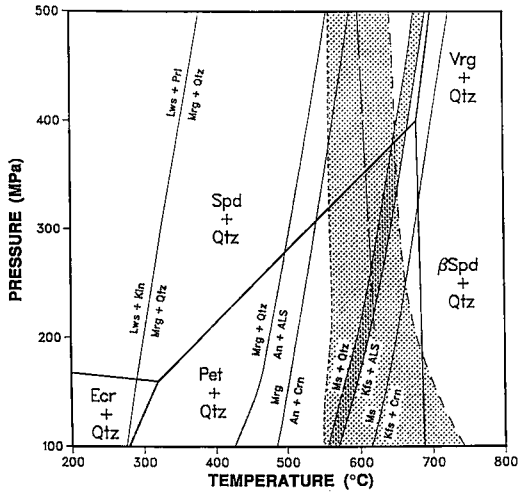

FIG. 2. A pressure - temperature diagram summarizing the equilibria relevant to the Harding pegmatite. The range of magmatic crystallization for the Harding pegmatite melt (broad shaded area) is bound at high temperature by the liquidus and at low temperature by the solidus as determined experimentally (Fenn 1986, Jahns 1982, Luth 1979) using splits of the same water-saturated bulk sample studied by Burnham & Jahns (1962), Jahns & Burnham (1969), and Vaughan (1963). The curve (long dashes) within the shaded region marks the beginning of crystallization of Li-Al-silicate, as calculated for the Harding pegmatite bulk sample (Burnham & Nekvasil 1986). The Li-Al-silicate phase diagram (bold lines) is from London (1984). The remaining equilibria curves (light lines) mark the formation of margarite + quartz [lawsonite + kaolinite = margarite + quartz + H_2O, lawsonite + pyrophyllite = margarite + quartz + H_2O (Chatterjee 1976)], the upper thermal stability limits of margarite + quartz and margarite [margarite + quartz = anorthite + Al_2SiO_5 + H_2O, margarite = anorthite + corundum + H_2O (Chatterjee 1976)], the breakdown of muscovite + quartz [muscovite + quartz = K-feldspar + Al_2SiO_5 + H_2O] (Kerrick 1972), and the upper thermal stability limit of muscovite [muscovite = K-feldspar + corundum + H_2O (Chatterjee & Johannes 1974)].

Pegmatite equilibria

Pegmatite magma. The bulk composition of the Harding pegmatite is granitic, as determined by analysis of a representative composite sample, reported in Jahns & Ewing (1976). Splits from this same sample, which represents one of the few good bulk samplings of a complex pegmatite, have been used in several experimental studies to determine the liquidus (Burnham & Jahns 1962), solidus (Vaughan 1963) and phase assemblages (Fenn 1986) as a function of pressure and temperature for a water-saturated Harding pegmatite magma. The results of these experiments have been discussed in Burnham (1979), Burnham & Nekvasil (1986), Fenn (1986), Jahns (1982), Jahns & Burnham (1969), and Luth (1979). The experimentally determined liquidus and solidus are nearly isothermal over the pressure range 200 to 500 MPa. For this range of pressure, the beginning of crystallization is 650 - 675°C, and the beginning of melting is approximately 550°C, making the interval of magmatic crystallization about 100°C (Fig. 2). The phase assemblages with decreasing temperature determined at 500 MPa by Fenn (1986) are remarkably similar to the sequence of zones observed in the pegmatite; compare the description of lithologic units in Table 1 with Figure 1 in Fenn (1986).

Li-Al-silicates. London (1984) has successfully demonstrated the use of the Li-Al-silicate phase diagram to constrain paths of crystallization for Li-rich pegmatites. The principal lithium aluminosilicate minerals in the Harding pegmatite are spodumene and eucryptite. Spodumene occurs in three different lithologic units, with a distinctive habit in each. The bulk of the spodumene occurs in the quartz - lath spodumene zone (see Table 1), where it forms long bladed euhedral crystals (Fig. 3a). The spodumene laths are locally subperpendicular to the hanging-wall contact, and at the base of the unit are arranged in a jackstraw fashion. Many crystals are bent and deformed, and in some exposures appear to wrap around blocks of lepidolite. Inward from the hanging-wall contact, the zonal assemblage spodumene + quartz appears abruptly at the base of the quartz zone. Spodumene is next most abundant in the microcline - spodumene zone, where it occurs as ovoid to irregularly shaped crystals intergrown along their margins with microcline (Table 1, Fig. 4). The third and least common occurrence of

TABLE 1. VERTICAL SUCCESSION OF LITHOLOGIC UNITS IN THE HARDING PEGMATITE*

BIOTITE + MUSCOVITE + QUARTZ ± GARNET ± MARGARITE ± SCHORL
A continuous metasomatic aureole, 3-100 cm, with a variable mineralogy dependent on the adjacent host-rock assemblage. The aureole is most prominent in the hanging-wall contact. Important accessory minerals include holmquistite, epidote and titanite.

QUARTZ + ALBITE + MUSCOVITE ± PERTHITE
A continuous wall zone containing a thin, 1-3 cm, border rind of quartz-albite-muscovite in contact with the metasomatic aureole. Beneath this rind is a continuous layer, 0.3-2 m, composed of a coarser aggregate of the same minerals. Beryl, columbite-tantalite, fluorapatite, and microcline are important accessory minerals. Beryl commonly occurs as huge (0.5-1 m) anhedral crystals, hence this zone is often called the beryl zone.

QUARTZ ± ALBITE ± MUSCOVITE
A continuous zone beneath the beryl zone, 0.5-10 m thick. Muscovite, microcline, and cleavelandite are minor accessory minerals.

QUARTZ + LATH SPODUMENE
A continuous zone, up to 14 m thick, in the thicker western portions of the main dike. This zone underlies the quartz zone and is composed of long bladed spodumene laths supported by a massive quartz matrix. The spodumene laths are arranged in a jack-straw fashion and locally are subperpendicular to the hanging-wall contact. Important accessory minerals occurring interstitial to spodumene laths include: beryl, fluorapatite, lepidolite, microcline, and microlite.

MICROCLINE + SPODUMENE + LEPIDOLITE + ALBITE + MUSCOVITE + QUARTZ
This unit forms an elongate lobe in the core of the thick western portion of the dike. The zone is 18 m in maximum thickness and 16-58 m wide. Down plunge, parallel to the dike, it extends for nearly 230 m. This zone is composed of an even-grained (1-10 cm) aggregate of primary quartz, microcline, spodumene, finer albite, and scattered millimeter-size uranium-rich microlite crystals. Lithium-bearing muscovite and lepidolite impregnate the microcline, coloring it pink. Locally this zone grades into pegmatite composed of lepidolite with spodumene; and with decreasing spodumene content, it grades into pure lepidolite replacement bodies. because of its common striking texture, this zone is often referred to as "spotted rock".

CLEAVELANDITE + ROSE MUSCOVITE ± QUARTZ
A replacement unit forming discontinuous masses marginal to the quartz - lath spodumene zone. Rose muscovite replaces spodumene and cleavelandite replaces quartz. Pseudomorphs of rose muscovite after spodumene are common.

CLEAVELANDITE + QUARTZ ± MUSCOVITE
A replacement unit forming highly discontinuous masses throughout the core and wall zone of the dike. Even-grained to radiating cauliflower masses of cleavelandite range from meter-size pods to extensive pseudomorphic zones.

BLOCKY PERTHITE ± QUARTZ ± ALBITE
This zone, dominated by large blocks (0.5-2 m) of cream to pale orange-colored perthitic microcline, occupies basal sections of the dike. Microcline crystals commonly contain fractures filled with albite aplite. This unit is continuous in the eastern extension of the dike and less so in the thick western portion.

QUARTZ + APLITIC ALBITE ± MUSCOVITE
This unit is continuous (up to 3 m thick) in all but the thinner parts of the dike, and also occurs as sporadic small patches (less than 0.5 m) in other units. Small pods of beryl (less than 0.5 m), infrequent columbite-tantalite crystals (less than 10 cm), and scattered quartz-spodumene aggregates (less than 4 cm) pseudomorphic after petalite are important accessories. Locally, veinlets of coarse platy lepidolite penetrate as fracture fillings.

* after Jahns & Ewing (1976, 1977), Chakoumakos (1978), Lumpkin *et al.* (1986)

spodumene is in the albite aplite unit. There, spodumene occurs as a symplectitic intergrowth with quartz, which together form pink ovoid aggregates scattered sparingly throughout the aplite unit in the main quarry area (Fig. 4). The symplectitic intergrowth of spodumene and quartz is characteristic of the decomposition of petalite, which has been described from several other localities; see reviews by London & Burt (1982), Černý (1975), and Černý & Ferguson (1972). Completing the spectrum of Li-Al-silicate occurrences in the Harding pegmatite, microcrystalline intergrowths of eucryptite + quartz after spodumene are common in the lower portions of the quartz – lath spodumene zone (Fig. 4).

The phase diagram for the Li-Al-silicates determined by London (1984) and the saturation of the Harding pegmatite magma with respect to Li-Al-silicate calculated by Burnham & Nekvasil (1986) are included in Figure 2. The initial crystallization of a Li-Al-silicate in the Harding pegmatite magma appears to have been petalite for a brief period, giving way to spodumene throughout the remaining period of magmatic crystallization. For the magma to become saturated with respect to Li-Al-silicate initially in the petalite field of stability and yet allow spodumene to predominate throughout the remainder of magmatic crystallization further constrains the initial isobaric P–T path to be no more than a few MPa above or below 350.

Micas. The occurrence and composition of micas in the pegmatite have been described by Lumpkin (1986) and Jahns & Ewing (1976). Muscovite is common in the wall zone, and Li-rich varieties occur throughout the other lithologic units. The occurrence of primary green muscovite in the border (rind) and main part of the beryl zone is consistent with pres-

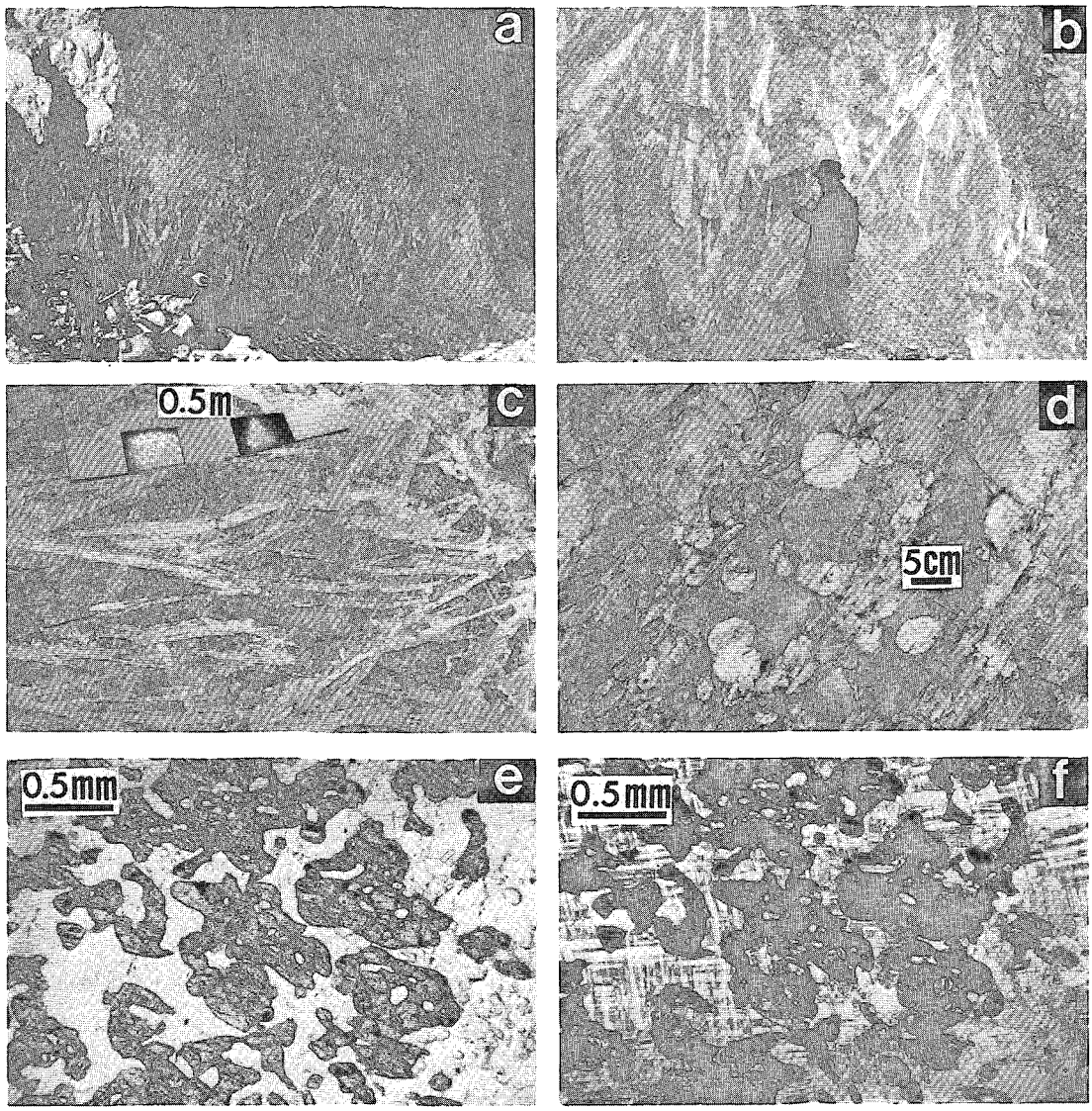

FIG. 3. Primary spodumene occurrences in the Harding pegmatite. a) Quarry wall *circa* 1944 exposing (from top to bottom) the amphibolite country-rock, the wall (beryl) zone, the quartz zone, and the quartz – lath spodumene zone. b) Detail of the giant-crystal texture of the quartz – lath spodumene zone. White, bladed spodumene crystals (up to 2 m long) are subperpendicular to the hanging-wall contact. c) Spodumene laths arranged in jackstraw fashion in an underground exposure at the base of the quartz – lath spodumene zone (1 to 2 m below the region shown in a). d) Outcrop view of a portion of the microcline – spodumene zone; the distinctive texture ("spotted rock") consists of spodumene orbs in a microcline matrix. e) Thin section photomicrograph (plane-polarized light) of the margin of a spodumene orb (center of orb is to the right of this view) from the microcline – spodumene zone ("spotted rock"). f) Same view (partly crossed polars) showing cross-hatch twinning in the microcline matrix. See text for further discussion.

sure on the order of 330–380 MPa, based on the upper stability of muscovite + quartz and $0.8 < X(H_2O) < 1.0$ (Fig. 2). In addition, compositions of the primary green muscovite have an average 5 mole % celadonite component (Lumpkin, in prep.), which extends the stability of muscovite in the granite system (Anderson & Rowley 1981). Lepidolite is common in the replacement units and the microcline

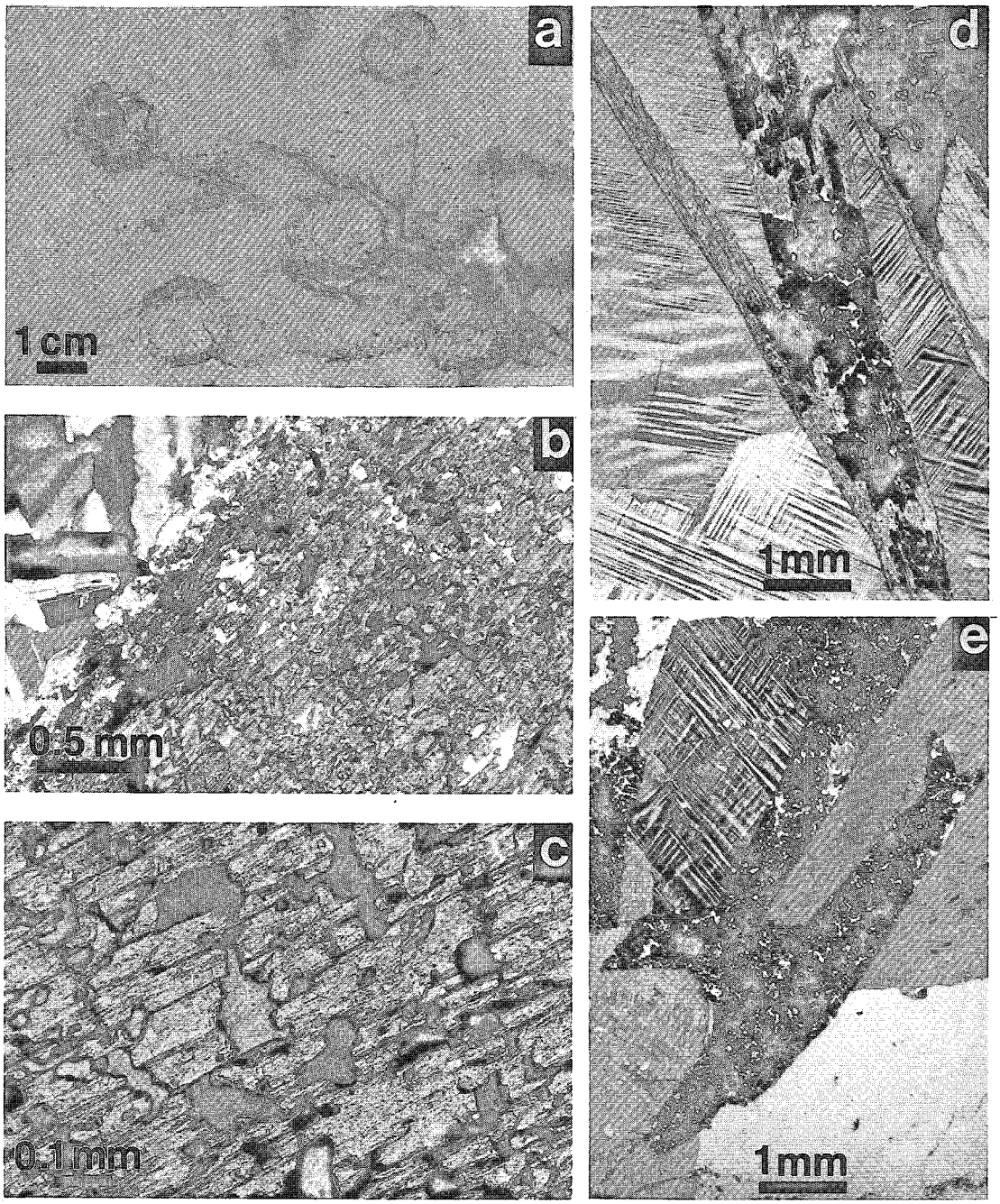

FIG. 4. Textures of replaced Li-Al-silicates in the Harding pegmatite. a) Hand sample view of pink spheroids, interpreted to be pseudomorphs after petalite, in albite aplite matrix from the basal aplite unit of the main dike. b) The pink spheroids are an intergrowth of spodumene and quartz with sharp boundaries against the albite aplite, as seen in thin section between crossed polars. c) An enlarged view shows that the spodumene in each spheroid is a continuous single crystal with quartz blebs scattered throughout. Groups of quartz blebs have the same optical orientation, suggesting that they are interconnected in the third dimension. d) Thin section view between crossed polars of eucryptite–quartz intergrowths (dark areas) partly replacing spodumene, set in a matrix of microcline. e) A similar photomicrograph showing spodumene crystals completely replaced by eucryptite + quartz. The latter two samples are from the quartz – lath spodumene zone exposed in the central adit penetrating the main dike.

spodumene zone. Biotite and Li–Be-bearing margarite are restricted to the metasomatic aureole. The occurrence of the Li–Be-bearing margarite is unusual and is being described by Chakoumakos & London (in prep.). For reference, the thermal stability of margarite and margarite + quartz are shown on Figure 2. However, the Li–Be-bearing brittle mica in the Harding aureole is a dioctahedral–trioctahedral intermediate, which probably has an enhanced thermal stability compared with ideal margarite. Given the uncertainty of the effects of the Li-for-□, Be-for-Al, and F-for-OH substitutions on the upper thermal stability of Li–Be-bearing margarite, the temperature of formation cannot be constrained; however, crystallization during subsolidus exomorphism would be consistent with an isobaric P–T path near 350 MPa.

Feldspars. Feldspars from several lithologic units of the pegmatite have been analyzed for major and minor elements by electron microprobe (Lumpkin 1986). A brief account of this study is given here as it relates to constraints on the P and T path of crystallization of the pegmatite. A detailed study of feldspars of the Harding pegmatite will be presented elsewhere (Lumpkin, in prep.). Two-feldspar pairs in apparent equilibrium were used to calculate temperatures according to the geothermometer of Whitney & Stormer (1977) and assuming a pressure of 300–400 MPa. For T calculations, only those feldspars were chosen that appeared, on the basis of textural observations, to be cogenetic. The temperatures determined for the quartz – lath spodumene zone, microcline – spodumene zone, and cleavelandite replacement units are in the range 325 to 485°C. These temperatures could reflect re-equilibration during pervasive albitization; however, the uncertainty of whether the feldspar pairs are truly cogenetic does not allow a confident interpretation of these temperatures.

Microcline from the microcline – spodumene zone displays pervasive cross-hatch twinning (see Fig. 3f), which implies a monoclinic precursor. The minimum temperature for the monoclinic-to-triclinic inversion in Or-rich alkali feldspars is about 500°C (Brown & Parsons 1989, Ribbe 1983). In the microcline – spodumene zone, perthite bulk compositions of approximately Or_{70-80} indicate primary crystallization at $T > 550$–575°C followed by exsolution of albite below this temperature, followed by the monoclinic-to-triclinic inversion of the Or-rich host at approximately 500°C, and final equilibration at about 350°C based on compositions of host microcline and exsolved albite.

Fluid inclusions. Fluid inclusions in quartz and beryl from the various lithologic units of the pegmatite were studied by Cook (1979); a preliminary analysis of these data was reported in Brookins *et al.* (1979). A revised analysis of Cook's data has been made (Lumpkin & Chakoumakos 1987, Chakoumakos & Lumpkin 1987) and is summarized more fully here. Using the compositions of fluid inclusions as determined by Cook (1979), isochores were calculated with the modified Redlich–Kwong equation of state presented by Bowers & Helgeson (1983a).

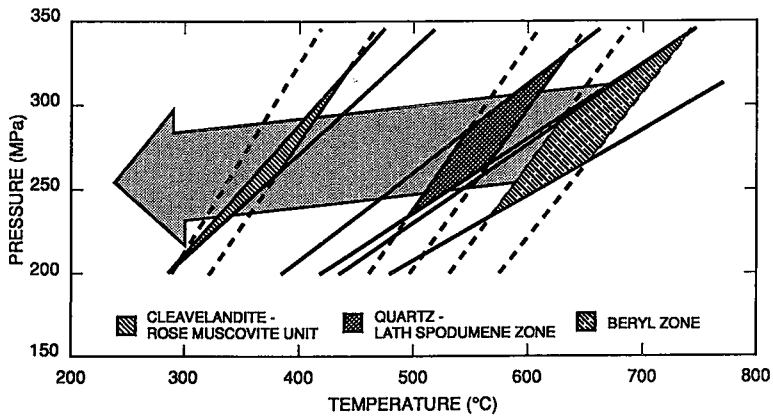

FIG. 5. Isochores for fluid inclusions in Harding pegmatite quartz and beryl. CO_2–H_2O isochores (solid lines) for the beryl zone (0.77–0.79 g/cm^3), quartz – lath spodumene zone (0.81–0.83 g/cm^3), and rose muscovite – cleavelandite unit (0.91–0.93 g/cm^3), including for each lithologic unit a range in $X(CO_2)$ of 0.75–1.0. CO_2–H_2O–NaCl isochores (dashed lines) (all 1.0–1.1 g/cm^3) for the beryl zone, quartz – lath spodumene zone, and rose muscovite – cleavelandite unit, including for each lithologic unit a range in $X(CO_2)$ of 0.0–0.1 and X(NaCl) of 0.0–0.1. The original data are from Cook (1979). The regions of intersection for the two types of isochores are shaded for each lithologic unit. The large shaded arrow shows the crystallization sequence.

For each lithologic unit, Cook determined inclusion compositions to be CO_2 only, CO_2–H_2O mixtures, and CO_2 – H_2O – NaCl-equivalent mixtures. This finding suggests that liquid–vapor immiscibility occurred during crystallization, that different compositions of fluid were trapped at different times during the course of crystallization, or that the inclusions have undergone various degrees of change in size or content since their formation. The calculations of Bowers & Helgeson (1983b) demonstrate that liquid–vapor immiscibilty in CO_2–H_2O–NaCl solutions can occur at temperatures as high as 400°C at 300 MPa. However, Sterner & Bodnar (1989) suggested that fluid inclusions in quartz under medium-grade metamorphic conditions may change in size as they re-equilibrate, in response to differential pressure during burial and subsequent uplift. London (1985) has examined fluid inclusions in spodumene + quartz assemblages that form from the breakdown of petalite in the Tanco pegmatite, and found that the *P* and *T* inferred from the inclusions in quartz are not consistent with the Li–Al-silicate phase diagram. Given that fluid inclusions in quartz may be suspect and that they constitute the bulk of the inclusions examined in the Harding pegmatite, we can only offer a cautious analysis of the fluid-inclusion data from the Harding pegmatite.

In general, the fluid inclusions indicate that the fluid composition (in mole %) evolved from $6CO_2$:4NaCl to less than $1CO_2$:10NaCl during the course of crystallization. Isochores for CO_2–H_2O inclusions display a progressive decrease in equilibration temperature from the beryl zone to the quartz – lath spodumene zone to the rose muscovite – cleavelandite unit, consistent with their sequence (wall zone to core) of crystallization or subsolidus re-equilibration. If the CO_2–H_2O and CO_2–H_2O–NaCl inclusions formed under the same conditions simultaneously, then for the various lithologic units the locus of intersections of the isochores for these two compositions should map the progressive change in *P* and *T* during crystallization of the pegmatite (Fig. 5). Despite the wide scatter and overlap of fluid densities, a progressive decrease in formation temperature following an approximately isobaric path is apparent for the primary lithologic units. This proposal is consistent with their inferred sequence of crystallization; however, the pressure indicated is

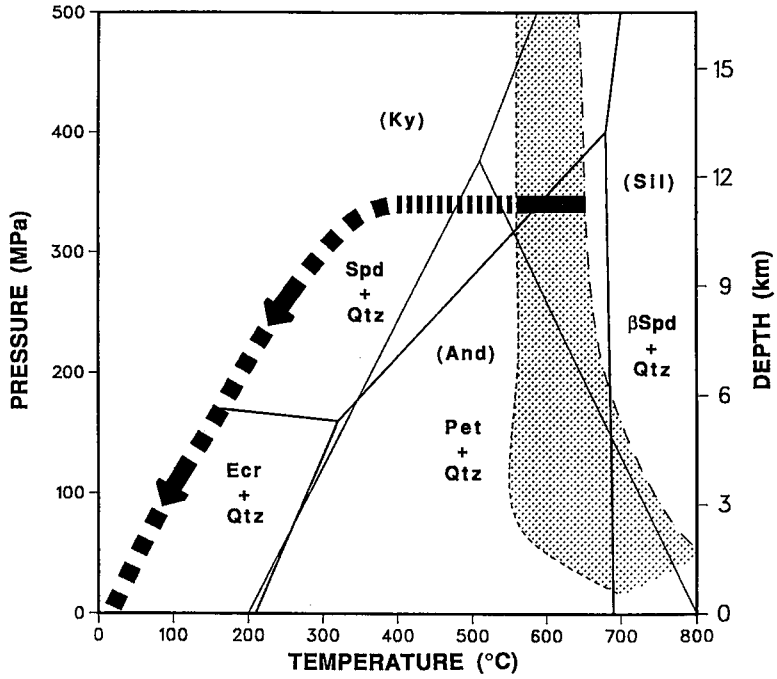

FIG. 6. Pressure – temperature path (bold curve) for the magmatic crystallization (solid line), hydrothermal stage (short-dashed line) and uplift (long-dashed curve) of the Harding pegmatite. Selected equilibria from Figures 1 and 2 also are shown and include the aluminosilicate phase diagram (solid lines), the Li–Al-silicate phase diagram (bold solid lines), and the liquidus (short-dashed line) and solidus (long-dashed line) of the water-saturated Harding pegmatite magma. The region of magmatic crystallization is shaded. See Figures 1 and 2 for references.

100–200 MPa lower than that consistent with the Li-Al-silicate phase diagram. See London (1985) for a similar appraisal of Cook's original findings.

Discussion

The predominant Li-Al-silicate in the Harding pegmatite is spodumene, but there is textural evidence of early-formed petalite. Its former presence suggests that the pegmatite magma must have become saturated with respect to Li-Al-silicate at a pressure slightly below or at the phase boundary between spodumene + quartz and petalite + quartz (Fig. 2). Furthermore, this pressure range of 330–350 MPa is consistent with the upper bound of 350 MPa provided by the peak regional metamorphic conditions. Because the pegmatite liquidus and solidus are nearly isothermal over the pressure range 330–350 MPa (11–12 km depth), the magmatic portion of crystallization began at ~650°C and continued isobarically to ~550°C (Fig. 6). The host-rock temperature at the time of intrusion could have been anywhere between 0 and 200°C below the pegmatite solidus temperature (*i.e.*, the temperature of the host rock must have been between the peak metamorphic conditions of 550°C and 350°C, the temperature at 11–12 km for a normal geothermal gradient of 30°C/km). Therefore, isobaric cooling through at least the magmatic stage is a reasonable assumption.

Given the available information, we can examine the cooling history of the Harding pegmatite magma using established mathematical theory (Lovering 1935, 1936, Carslaw & Jaeger 1959, Jaeger 1964). Of interest are the maximum temperature

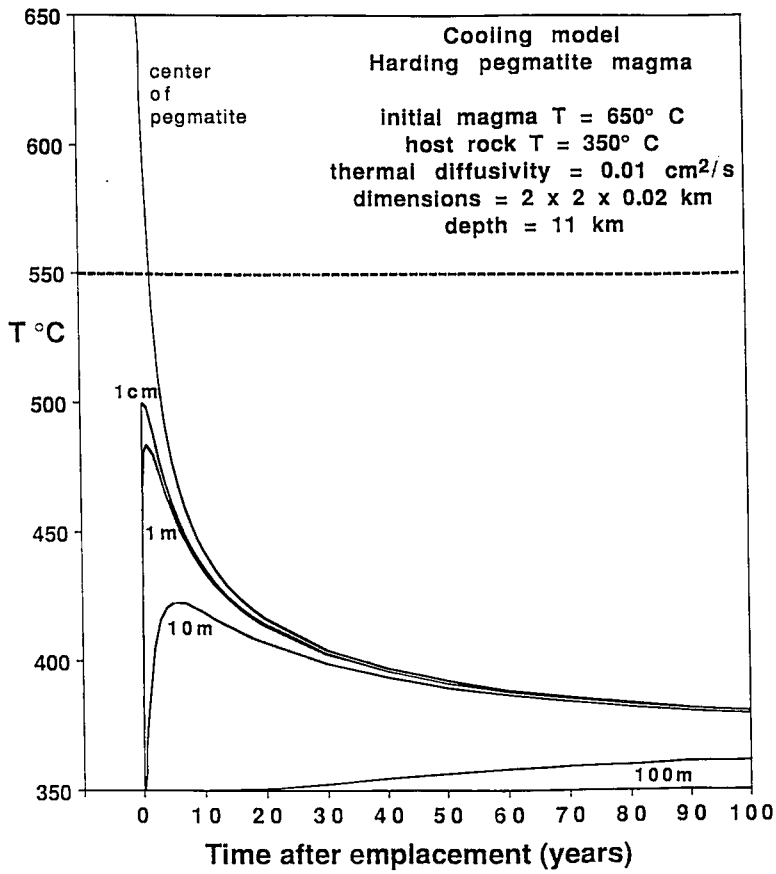

Fig. 7. Model thermal history of the center of the pegmatite and positions within the aureole 1 cm, 1 m, 10 m, and 100 m above the hanging-wall contact. The general character of the curves is the same for higher temperatures of the host rock and a range of thermal diffusivities (0.02 - 0.005 cm^2/s). The solidus of the pegmatite magma and the peak metamorphic temperature, both at 550°C, are marked by the dashed line.

experienced by the aureole, and the time required for the magma body to thermally equilibrate with the host rock. As noted by Jaeger (1964), a realistic theory requires detailed knowledge about the intrusion (emplacement rate, geometry and dimensions of the magma chamber, depth of cover), the magma (initial temperature, thermal diffusivity, heat of crystallization, temperature range of crystallization), and the host rock (initial temperature, thermal diffusivity, geothermal gradient). Further complications include the thermal effects of volatiles in the host rock, of volatiles or convection in the magma, heterogeneous texture or differentiation during the progress of crystallization, and heat production due to radioactivity. Much of the necessary information has been established in the previous section or can be reasonably estimated. A simplified model has been chosen to illustrate the important general features. Consider the cooling of a parallelepiped body of magma of width $2d$ and length $2l$ at a depth h_1 below the surface and with its lower surface at depth h_2. If the magma, initially at temperature T_1, is injected into country rock at temperature T_0, the temperature at any position (x, y, z) at time t is

$$T(x,y,z,t) = T_0 + \tfrac{1}{8}(T_1-T_0)\{\mathrm{erf}[(x+d)/2(\varkappa t)^{1/2}]-\mathrm{erf}[(x-d)/2(\varkappa t)^{1/2}]\}\{\mathrm{erf}[(y+l)/2(\varkappa t)^{1/2}]-\mathrm{erf}[(y-l)/2(\varkappa t)^{1/2}]\}\{\mathrm{erf}[(z+h_1)/2(\varkappa t^{1/2}]-\mathrm{erf}[(z-h_2)/2(\varkappa t)^{1/2}]+\mathrm{erf}[(z+h_1)/2(\varkappa t)^{1/2}]-\mathrm{erf}[(z+h_2)/2(\varkappa t)^{1/2}]\}$$

(Carslaw & Jaeger 1959). Underlying assumptions are that the thermal diffusivities ($\varkappa$) of the magma, subsolidus assemblage, and the host rock are the same, and that the thermal contribution from the heat of crystallization is negligible.

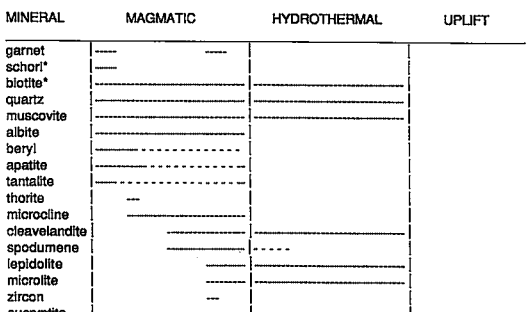

FIG. 8. Crystallization sequence of major and minor minerals in the Harding pegmatite and its metasomatic aureole. The magmatic, hydrothermal, and uplift stages of crystallization correspond to the crystallization path shown in Figure 6. Minerals marked with an asterisk occur only in the metasomatic aureole.

First, assume instantaneous emplacement of the pegmatite magma at the temperature of the liquidus, 650°C. At the beginning of crystallization, the igneous body is a parallelepiped with dimensions 2 × 2 × 0.02 km and oriented such that this finite sheet is parallel with the surface. The depth to the upper surface of the body is 11 km. The thermal diffusivity is assumed to be everywhere the same at 0.01 cm^2/s. Cooling curves for the center of the pegmatite and positions within the aureole are shown in Figure 7 for a host-rock temperature of 350°C. The magma cools quickly while the contact heats rapidly to a maximum of $\frac{1}{2}(T_1-T_0)$. Any point in the aureole heats to a maximum temperature (diminishing with distance) and then cools gradually. For higher host-rock temperatures, the general character of the cooling curves is the same. For host-rock temperatures below 550°C, the magmatic crystallization (giant-crystal texture) would have occurred in 100 years or less. For a host-rock temperature near the pegmatite solidus (550°C), the magmatic portion of crystallization would have taken much longer (> 1000 years).

The subsolidus hydrothermal replacement and reequilibration (*i.e.*, "stewing in its juices"; Jahns 1982) continued for several million years. Nearly isobaric cooling continued to 400–300°C, followed by uplift and erosion (Fig. 6). The decompression is shown to follow a 30°C/km geotherm, although the average slope of the fluid-inclusion isochores might indicate an initially greater change in pressure for the uplift trajectory. Given the estimated age and depth of the pegmatite, the average uplift rate of the Picuris Range is inferred to have been 0.7 – 1.0 cm/yr.

Figure 8 summarizes the crystallization sequence for the important minerals of the Harding pegmatite and its aureole. Early in the magmatic stage, major concentrations of beryl and columbite–tantalite crystallized in the wall zone at 650 – 625°C. Quartz–spodumene intergrowths exposed in footwall aplite are interpreted as pseudomorphic replacements of early-formed petalite. Microlite crystallized in association with spodumene late in the magmatic stage at 575 – 550°C. Additional microlite formed during the hydrothermal stage, as extensive masses of cleavelandite, muscovite and lepidolite replaced pre-existing pegmatite. Pseudomorphs of rose muscovite after spodumene laths and casts of beryl crystals in lepidolite masses are irrefutable evidence that previously solid pegmatite has been replaced (Chakoumakos 1978). Li–Be-bearing margarite, prominent in the hanging-wall metasomatic aureole, probably crystallized below the pegmatite solidus. In support of this contention, London (1986) noted that the mineral assemblages of the metasomatic aureole are characteristic of greenschist-facies metamorphic conditions (*i.e.*, temperatures); thus the infiltration of

pegmatitic fluids into the host rock that gave rise to the aureole must have occurred at subsolidus temperatures. The inferred *P–T* path in Figure 6 suggests that most of the eucryptite replacement of spodumene occurred during uplift at 100–200°C.

ACKNOWLEDGEMENTS

We are grateful to Art Montgomery and the University of New Mexico for their successful efforts to preserve the Harding pegmatite mine as a classic locality for teaching and research. Special tribute goes to the Griego family, whose dedicated service to the Harding mine now spans three generations. The photographs appearing as Figures 3a and 3b were kindly provided by Art Montgomery. We are grateful for constructive reviews by Petr Černý, David London, and Robert Meintzer. This research was conducted while BCC was a Postdoctoral Fellow supported by the U. S. Department of Energy, Basic Energy Sciences, under grant DE-FG04-84ER45099 (R. C. Ewing, principal investigator).

REFERENCES

ANDERSON, J.L. & ROWLEY, M.C. (1981): Synkinematic intrusion of peraluminous and associated metaluminous granitic magmas, Whipple Mountains, California. *Can. Mineral.* **19**, 83-101.

BAUER, P.W. (1984): Stratigraphic summary and structural problems of Precambrian rocks, Picuris Range, New Mexico. *In* New Mexico Geol. Soc., 35th Field Conf., Guidebook (W.S. Baldridge, P.W. Dickerson, R.E. Riecker & J. Zidek, eds.), 199-204.

BOWERS, T.S. & HELGESON, H.C. (1983a): Calculation of the thermodynamic and geochemical consequences of nonideal mixing in the system H_2O–CO_2–NaCl on phase relations in geologic systems: equation of state for H_2O–CO_2–NaCl fluids at high pressures and temperatures. *Geochim. Cosmochim. Acta* **47**, 1247-1275.

_____ & _____ (1983b): Calculation of the thermodynamic and geochemical consequences of nonideal mixing in the system H_2O–CO_2–NaCl on phase relations in geologic systems: metamorphic equilibria at high pressures and temperatures. *Am. Mineral.* **68**, 1059-1075.

BROOKINS, D.G., CHAKOUMAKOS, B.C., COOK, C.W., EWING, R.C., LANDIS, G.P. & REGISTER, M.E. (1979): The Harding pegmatite: summary of recent research. *In* New Mexico Geol. Soc., 30th Field Conf., Guidebook (R.V. Ingersoll & L.A. Woodward, eds.), 127-133.

BROWN, W.L. & PARSONS, I. (1989): Alkali feldspars: ordering rates, phase transformations and behaviour diagrams for igneous rocks. *Mineral. Mag.* **53**, 25-42.

BURNHAM, C.W. (1979): Magmas and hydrothermal fluids. *In* Geochemistry of Hydrothermal Ore Deposits (H.L. Barnes, ed.). Wiley, New York, 71-136.

_____ & JAHNS, R.H. (1962): A method for determining the solubility of water in silicate melts. *Am. J. Sci.* **260**, 721-745.

_____ & NEKVASIL, H. (1986): Equilibrium properties of granite pegmatite magmas. *Am. Mineral.* **71**, 239-263.

CARSLAW, H.S. & JAEGER, J.C. (1959): *Conduction of Heat in Solids* (2nd ed.). Oxford University Press, New York.

ČERNÝ, P. (1975): Granitic pegmatites and their minerals: selected examples of recent progress. *Fortschr. Mineral.* **52**, 225-250.

_____ & FERGUSON, R.B. (1972): The Tanco pegmatite at Bernic Lake, Manitoba. IV. Petalite and spodumene relations. *Can. Mineral.* **11**, 660-678.

CHAKOUMAKOS, B.C. (1978): *Microlite, the Harding pegmatite, Taos County, New Mexico*. B.S. thesis, Univ. New Mexico, Albuquerque, New Mexico.

_____ & LUMPKIN, G.R. (1987): Constraints on the crystallization of the Harding pegmatite, Taos County, New Mexico. *Geol. Assoc. Can. - Mineral. Assoc. Can., Program Abstr.* **12**, 30.

CHATTERJEE, N.D. (1976): Margarite stability and compatibility relations in the system CaO - Al_2O_3 - SiO_2 - H_2O as a pressure-temperature indicator. *Am. Mineral.* **61**, 699-709.

_____ & JOHANNES, W. (1974): Thermal stability and standard thermodynamic properties of synthetic $2M_1$ muscovite, $KAl_2[AlSi_3O_{10}(OH)_2]$. *Contrib. Mineral. Petrol.* **48**, 89-114.

CLARK, G.S. (1982): Rubidium–strontium systematics of complex granitic pegmatites. *In* Granitic Pegmatites in Science and Industry (P. Černý, ed.). *Mineral. Assoc. Can., Short Course Handbook* **8**, 347-371.

COOK, C.W. (1979): *Fluid Inclusions and Petrogenesis of the Harding Pegmatite, Taos County, New Mexico*. M.S. thesis, Univ. New Mexico, Albuquerque, New Mexico.

FENN, P.M. (1986): On the origin of graphic granite. *Am. Mineral.* **71**, 325-330.

GANGULY, J. (1969): Chloritoid stability and related parageneses: theory, experiments and applications. *Am. J. Sci.* **267**, 910-944.

GRAMBLING, J.A. (1986): Crustal thickening during Proterozoic metamorphism and deformation in New Mexico. *Geology* **14**, 149-152.

_____ & WILLIAMS, M.L. (1985): The effects of Fe^{3+} and Mn^{3+} on aluminum silicate phase relations in north-central New Mexico, U.S.A. *J. Petrol.* **26**, 324-354.

HIRSCHBERG, A. & WINKLER, H.G.F. (1968): Stabilitätsbeziehungen zwischen Chlorit, Cordierit und Almandin bei der Metamorphose. *Contrib. Mineral. Petrol.* **18**, 17-42.

HOLCOMBE, R.J. & CALLENDER, J.F. (1982): Structural analysis and stratigraphic problems of Precambrian rocks of the Picuris Range, New Mexico. *Geol. Soc. Am. Bull.* **93**, 138-149.

HOLDAWAY, M.J. (1978): Significance of chloritoid-bearing and staurolite-bearing rocks in the Picuris Range, New Mexico. *Geol. Soc. Am. Bull.* **89**, 1404-1414.

_____ (1971): Stability of andalusite and the aluminum silicate phase diagram. *Am. J. Sci.* **271**, 97-131.

JAEGER, J.C. (1964): Thermal effects of intrusions. *Rev. Geophys.* **2**, 443-466.

JAHNS, R.H. (1982): Internal evolution of granitic pegmatites. *In* Granitic Pegmatites in Science and Industry (P. Černý, ed.). *Mineral. Assoc. Can., Short Course Handbook* **8**, 293-328.

_____ & BURNHAM, C.W. (1969): Experimental studies of pegmatite genesis. I. A model for the derivation and crystallization of granitic pegmatites. *Econ. Geol.* **64**, 843-864.

_____ & EWING, R.C. (1976): The Harding mine, Taos County, New Mexico. *In* New Mexico Geol. Soc., 27th Field Conf., Guidebook (R.C. Ewing & B.S. Kues, eds.), 263-276.

_____ & _____ (1977): The Harding mine, Taos County, New Mexico. *Mineral. Rec.* **8**, 115-126.

KERRICK, D.M. (1972): Experimental determination of muscovite + quartz stability with $P(H_2O) < P(total)$. *Am. J. Sci.* **272**, 946-958.

LONDON, D. (1984): Experimental phase equilibria in the system $LiAlSiO_4 - SiO_2 - H_2O$: a petrogenetic grid for lithium-rich pegmatites. *Am. Mineral.* **69**, 995-1004.

_____ (1985): Origin and significance of inclusions in quartz: a cautionary example from the Tanco pegmatite, Manitoba. *Econ. Geol.* **80**, 1988-1995.

_____ (1986): Holmquistite as a guide to pegmatitic rare metal deposits. *Econ. Geol.* **81**, 704-712.

_____ & BURT, D.M. (1982): Lithium aluminosilicate occurrences in pegmatites and the lithium aluminosilicate phase diagram. *Am. Mineral.* **67**, 483-493.

LONG, P.E. (1974): Constrasting types of Precambrian granitic rocks in the Dixon–Peñasco area, northern New Mexico. *In* New Mexico Geological Society, 25th Field Conf., Guidebook (C.S. Siemers, ed.), 101-108.

LOVERING, T.S. (1935): Theory of heat conduction applied to geological problems. *Geol. Soc. Am. Bull.* **46**, 69-94.

_____ (1936): Heat conduction in dissimilar rocks and the use of thermal models. *Geol. Soc. Am. Bull.* **47**, 87-100.

LUMPKIN, G.R. (1986): Electron microprobe analysis of feldspars and micas from the Harding pegmatite, Taos County, New Mexico. *Int. Mineral. Assoc., 14th Gen. Meet.*, 161 (abstr.).

_____ & CHAKOUMAKOS, B.C. (1987): Crystallization and economic mineralogy of the Harding pegmatite, Taos County New Mexico. *Geol. Soc. Am., Abstr. Programs* **19**, 61.

_____, _____ & EWING, R.C. (1986): Mineralogy and radiation effects of microlite from the Harding pegmatite, Taos County, New Mexico. *Am. Mineral.* **71**, 569-588.

LUTH, W.C. (1979): Melting and crystallization relations in the Harding, New Mexico pegmatite bulk composition. *New Mexico Mineral Symp.*, Univ. New Mexico, Albuquerque, New Mexico, 3 (abstr.).

MCCARTY, R.M. (1983): *Structural Geology and Petrography of Part of the Vadito Group, Picuris Mountains, New Mexico.* M.S. thesis, Univ. New Mexico, Albuquerque, New Mexico.

RIBBE, P.H. (1983): Aluminum–silicon order in feldspars; domain textures and diffraction patterns. *In* Feldspar Mineralogy, 2nd edition (P.H. Ribbe, ed.). *Rev. Mineral.* **2**, 21-55.

STERNER, S.M. & BODNAR, R.J. (1989): Synthetic fluid inclusions. VII. Re-equilibration of fluid inclusions in quartz during laboratory simulated metamorphic burial and uplift. *J. Metamorphic Geol.* **7**, 243-260.

VAUGHAN, D.E.W. (1963): *The Crystallization Ranges of the Spruce Pine and Harding Pegmatites.* M.S. thesis, Pennsylvania State Univ., University Park, Pennsylvania.

WHITNEY, J.A. & STORMER, J.C., JR. (1977): The distribution of $NaAlSi_3O_8$ between coexisting microcline and plagioclase and its effect on geothermometric calculations. *Am. Mineral.* **62**, 687-691.

Received October 31, 1989, revised manuscript accepted February 28, 1990.